

Science with SIRTf – Some Examples

Bernhard Brandl and the IRS Team

*Cornell University, 222 Space Sciences Building, Ithaca, NY 14853,
USA*

Abstract. The Space InfraRed Telescope Facility (SIRTf) is a spaceborne, cryogenically-cooled infrared observatory capable of studying objects ranging from our Solar System to the distant reaches of the Universe. SIRTf is the final element in NASA’s Great Observatories Program, and an important component of its Origins Program. The intent of this paper is to summarize the most important parameters of the observatory and its scientific instruments and to present three typical examples of scientific areas where SIRTf will have a significant impact. These examples of “nearby” targets – brown dwarf surveys, protostellar disks, and massive young clusters – have been selected in regard to the main topics of this conference.

1. Introduction

The Space InfraRed Telescope Facility (SIRTf) (Fanson et al. 1998) is the fourth and final element in NASA’s family of “Great Observatories”. SIRTf consists of a 0.85-meter telescope, cooled to $T < 5.5K$ and three cryogenically-cooled science instruments capable of performing imaging and spectroscopy in the 3 – 180 μ m wavelength range (Fig. 1). More details are summarized in Table 1.

Launch Date	December 2001
Launch Vehicule/Site	Delta 7920H ELV / Kennedy Space Center
Estimated Lifetime	2.5 years (minimum); 5+ years (goal)
Orbit	Earth-trailing, Heliocentric
Wavelength Coverage	3 - 180 microns
Telescope	85 cm diameter, f/12 lightweight Beryllium
Diffraction Limit	6.5 microns
Science Capabilities	Imaging / Photometry, 3-180 microns Spectroscopy, 5-40 microns Spectrophotometry, 50-100 microns
Planetary Tracking	1 arcsec / sec
Cryogen / Volume	Liquid Helium / 360 liters
Launch Mass	950 kg

Table 1. Summary of important SIRTf parameters

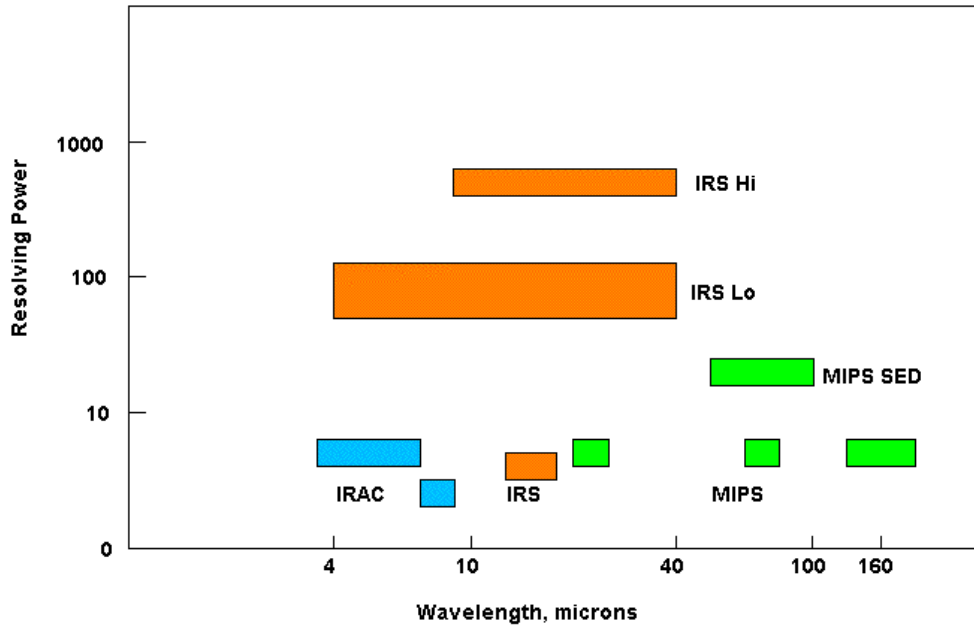


Figure 1. Wavelength versus spectral resolution coverage of the scientific instruments onboard SIRTf.

Incorporating large-format infrared detector arrays, SIRTf offers orders-of-magnitude improvements in capability over existing programs. While SIRTf's mission lifetime requirement remains 2.5 years, recent programmatic and engineering developments have brought a 5-year cryogenic mission within reach. A fast-track development schedule will lead to a launch in December 2001. SIRTf represents an important scientific and technical bridge to NASA's new Origins program.

75% of the observing time will be available to the community in form of general science proposals and so-called Legacy proposals (The SIRTf Legacy Science Program is intended to maximize the scientific return from SIRTf early in the mission, and comprises a handful of large-scale observing projects to be executed primarily within the first year of SIRTf's lifetime.) In addition for the first 2.5 years of SIRTf's prime mission, 20 percent of observing time will be allocated to the GTO program and an additional 5% is reserved as Director's discretionary time. More details can be found at <http://sirtf.caltech.edu>

This paper presents three examples of "typical" SIRTf science, most of which are covered by the GTO program. These examples have been selected to demonstrate SIRTf's superb capabilities and to match the scientific focus of the 3rd "Three Island Euroconference on Clusters and Associations". More examples can be found elsewhere, e.g., in Brandl et al. (1999).

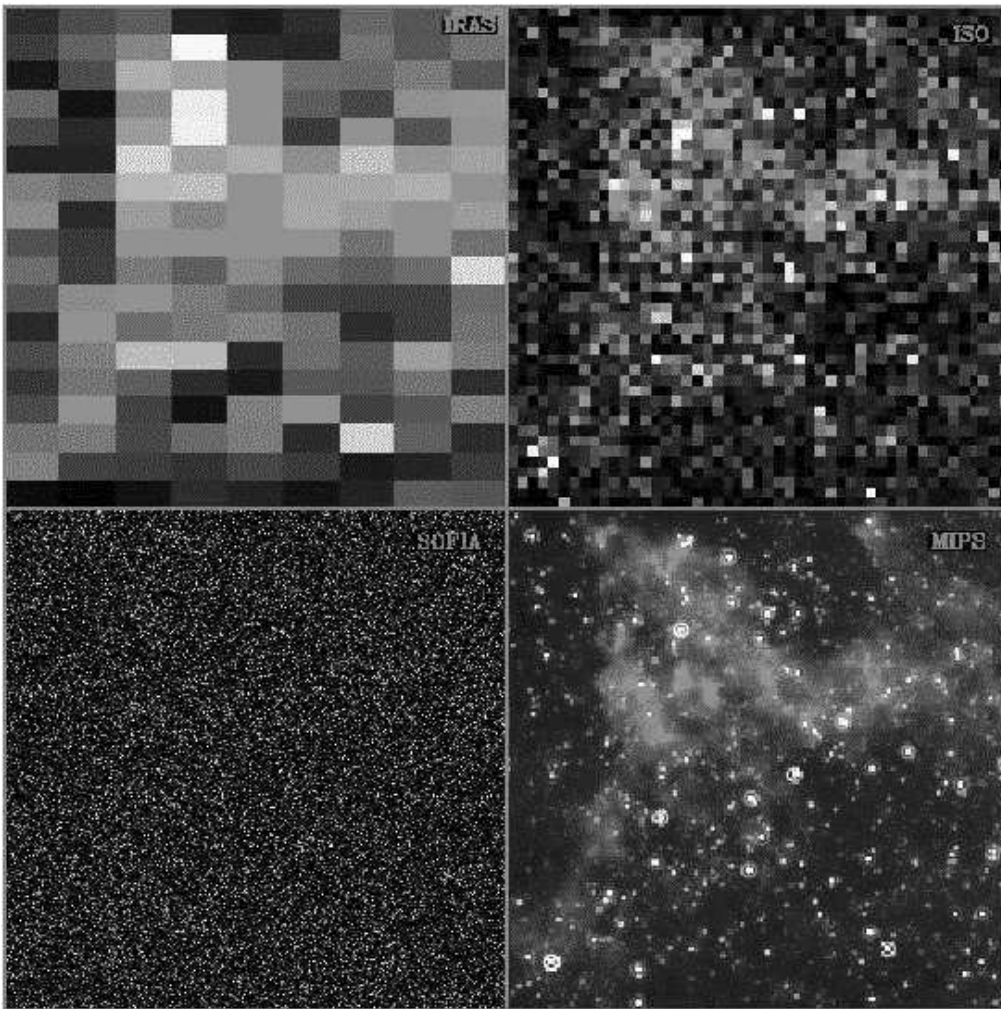


Figure 2. These are logarithmically scaled versions of comparison images generated for IRAS, ISO, SOFIA, and MIPS. A test field was "observed" with these four instruments, giving each instrument 24 hours of integration time and taking into account the sensitivity, the plate scale, and the field of view. The IRAS image has very large pixels and is really only capable of detecting the infrared cirrus in this field. The ISO image has better spatial resolution but is limited by the small field-of-view and low sensitivity of the arrays. SOFIA has excellent spatial resolution because of the large (2.5m) telescope but a correspondingly small field-of-view (even with a 32x32 array) and is limited in sensitivity because it uses warm optics. The predicted MIPS performance on the test field is excellent because of the high sensitivity of the detectors, good spatial resolution, and the large field-of-view of the 32x32 array. (Engelbracht et al. 1999).

2. Instruments and Sensitivities

SIRTF's science payload consists of three cryogenically cooled instruments, which together offer observational capabilities stretching from the near- to the far-infrared. Figure 2 shows a simulation comparing the performance of the latest major IR observatories on deep large area surveys. Following is a brief summary of the characteristics of each instrument. Details are described in the SIRTF Observers Manual (2000).

2.1. The InfraRed Array Camera (IRAC)

The IRAC (Giovanni G. Fazio, PI) provides images at 3.6, 4.5, 5.8 and 8.0 μm , over two adjacent 5.12 x 5.12 arcminute fields of view. One field of view images simultaneously at 3.6 and 5.8 μm and the other at 4.5 and 8.0 μm via a dichroic beamsplitter. All four detector arrays are 256x256 with 1.2 arcsecond square pixels. A cold shutter is provided for dark measurements, and also allows the detectors to be illuminated by light from a transmission calibrator. Sensitivities for IRAC are given in Table 2.

waveband [μm] (center wavelength)	sensitivity [μJy] (1σ in 100s)	saturation [Jy] (0.4s, point source)
3.6	1.29	1.39
4.5	1.86	1.19
5.8	6.09	2.05
8.0	7.97	1.35

Table 2. IRAC point source sensitivities and saturation flux densities

2.2. The InfraRed Spectrograph(IRS)

The IRS (James R. Houck, PI) performs both low and high-resolution spectroscopy. Low resolution, long slit spectra ($\lambda/\Delta\lambda = 62 - 124$) can be obtained from 5.3 to 40 μm . High resolution spectra ($\lambda/\Delta\lambda = 600$) in Echelle mode can be obtained from 10 to 37 μm . The spectrograph consists of four modules, each of which is built around a 128x128 pixel array. The sizes of the slits are summarized in table 3.

wavelength range [μm]	resolution [$\lambda/\Delta\lambda$]	pixel size ["]	slit width ["]	slit length ["]
5.3 - 8.5	62 - 124	1.8	3.6	54.6
7.5 - 14.2	62 - 124	1.8	3.6	54.6
14.2 - 21.8	62 - 124	4.8	9.7	151.3
20.6 - 40.0	62 - 124	4.8	9.7	151.3
10.0 - 19.5	600	2.4	5.3	11.8
19.3 - 37.0	600	4.8	11.1	22.4

Table 3. Slit sizes of the different IRS modules

One of the modules incorporates a peak-up function that can be used in locating and positioning sources on any of the four spectrometer slits with sub-arcsecond precision. The peak-up array has 1.8 arcsec square pixels and a field

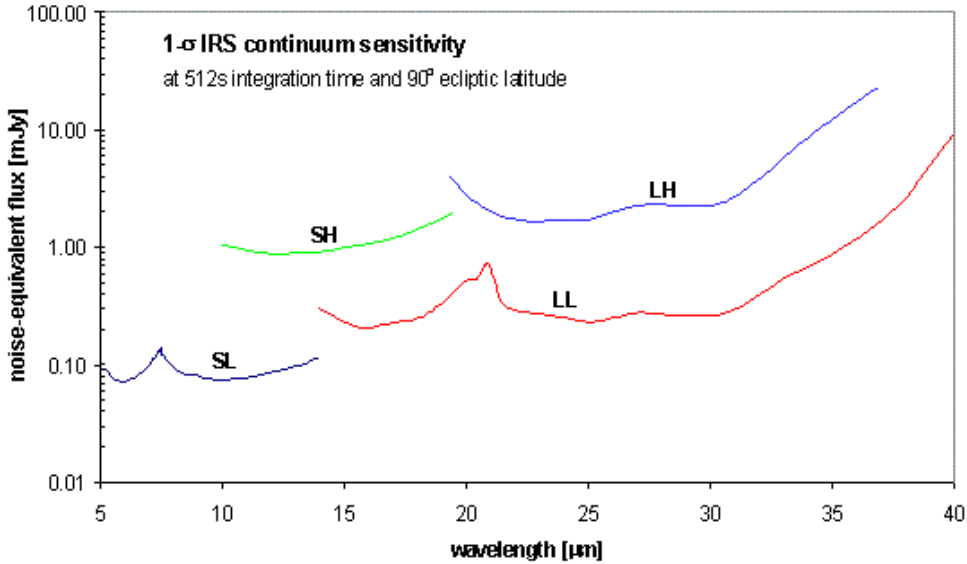


Figure 3. 1σ continuum sensitivity of all four IRS modules in a 512 second integration time and 90° ecliptic latitude as a function of wavelength.

of view of 1 arcminute by 1.2 arcminutes. Two filters are available for use with up array, covering 13.5 – 18.5 microns or 18.5 – 26 microns. Sensitivities for the IRS are shown in Figure 3.

2.3. The Multiband Imaging Photometer for SIRTf (MIPS)

The MIPS (George H. Rieke, PI) is designed to provide photometry and super resolution imaging as well as high speed mapping capabilities in three wavelength bands centered near 24, 70 and 160 microns. The array materials are Si:As, Ge:Ga, and stressed Ge:Ga with pixel sizes of 2.5, 5, 10, and 16 arcseconds, depending on wavelength and detector. MIPS is also capable of low-resolution spectroscopy ($\lambda/\Delta\lambda = 15 - 25$) over the wavelength range 55-96 microns and a Total Power Mode for measuring absolute sky brightness. Sensitivities for MIPS are given in Table 4.

waveband [μm] (center wavelength)	sensitivity [mJy] (5σ in 500s)	saturation [Jy] (1s, point source)
24	0.35	13
70	1.30	9
SED	6.50	45
160	22.5	40

Table 4. MIPS point source sensitivities and saturation flux densities

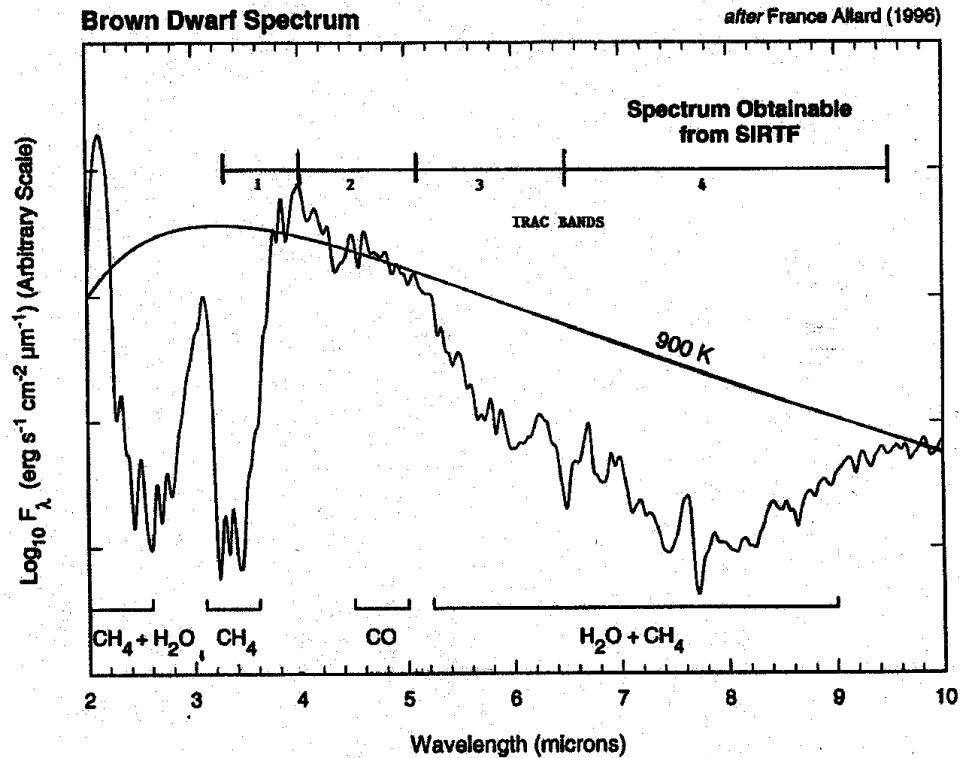


Figure 4. The IRAC bands are shown in relation to a model brown dwarf spectrum (Allard et al. 1996) and a 900K blackbody.

3. Science with SIRTF

3.1. Example 1: Searches for Brown Dwarfs

During the past two years, ground-based surveys have begun to succeed in identifying large numbers of relatively young, nearby brown dwarfs in star-forming regions, young open clusters and the old. IRAC will be able to extend those efforts to older and lower mass brown dwarfs and superplanets. In nearby star-forming regions like Taurus, IRAC should be able to detect isolated objects down to near the mass of Jupiter, $1M_J$. In the nearest and best-studied open clusters – in particular, the Pleiades and the Hyades – IRAC should be able to detect brown dwarfs down to $10M_J$.

As Figure 4 illustrates, the ratio of the IRAC bands at 3.6 and $4.5\mu\text{m}$ is a very good means of selecting brown dwarfs. The method of observation would be to carry out a large area survey of several open star clusters (e.g. NGC 2264, Pleiades, Hyades). The survey area is approximately 5 square degrees for NGC 2264 and the Pleiades, and approximately 10 square degrees for the Hyades. The integration time would be 30 seconds per position, observing each position three times (90s total), which would achieve a sensitivity of $10\mu\text{Jy}$, 5σ at $4.5\mu\text{m}$. The total observing time for all three fields would be about 160

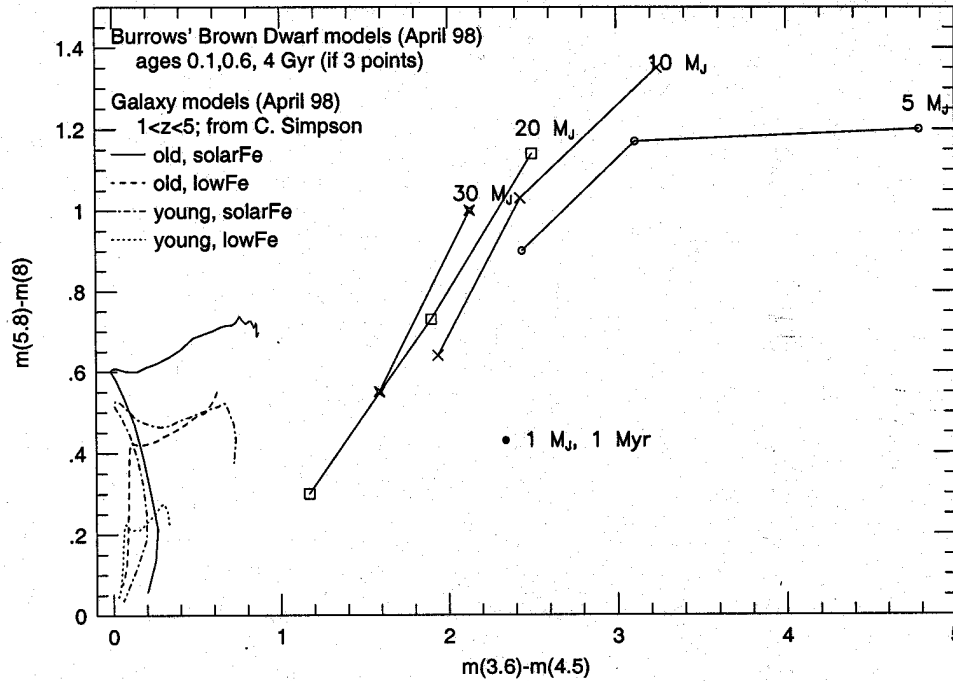


Figure 5. IRAC color/color diagram showing galaxies (lower left corner) and brown dwarfs of different masses and ages (upper right). (Fazio et al. 1999 and references therein).

hours. The brown dwarf candidates would be selected by $3.6/4.5\mu\text{m}$ color, based on model predictions and known objects from the 2MASS and DENIS surveys. The lowest mass objects will be detected only at $4.5\mu\text{m}$ in 90s. The $4.5\mu\text{m}$ only objects would need to be re-observed with much longer integrations to provide a detection at $3.6\mu\text{m}$.

Figure 5 shows the IRAC color/color diagram for objects with masses of 5, 10, 20, and $30M_J$ at various ages. The IRAC color/color diagram for galaxies in the field is shown in the same diagram. The galaxies are well-separated from the brown dwarfs, appearing in the lower left corner of the color/color plot. (Fazio et al. 1999).

3.2. Example 2: Protostellar and Protoplanetary Disks

The spectral range covered by the IRS includes most of the important emission and absorption features from interstellar and solar-system-like dust grains (Fig. 6). It also includes many fine structure lines of ions and neutral atoms that are bright in H II regions, phot-dissociation regions and young stellar objects; the lower transitions in pure rotational spectrum of molecular hydrogen; and many other molecular rotational and rotation-vibration lines of abundant species whose emission is important in the energetics or diagnosis of warm molecular gas.

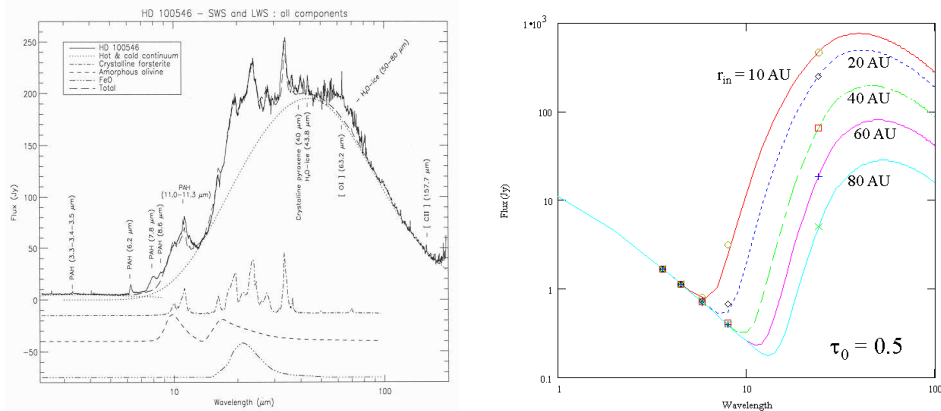


Figure 6. Left: ISO-SWS/LWS spectrum of the Herbig Ae star HD 100546 (Malfait et al. 1998). Note the wealth of spectral features including PAHs (polycyclic aromatic hydrocarbons), amorphous and crystalline silicates, rust, etc. The continuum cutoff marks the disk’s inner edge. Right: Model debris disks made with HR4796A-like parameters ($L = 18.1L_{\odot}$, $T_{\star} = 9000K$, $D = 67pc$, $r_{outer} = 100$ AU). The plot symbols indicate positions of the IRAC and MIPS $24\mu m$ bands. The further out the inner radius of the disk the fainter its radiation relative to the stellar continuum at shorter wavelengths.

The IRS is particularly sensitive to emission from dust and gas that lies in the inner parts of protostellar, protoplanetary and debris disks, between a few tenths and a few tens of AU from the star. In the nearest regions of star formation, the IRS will be able – in just a few minutes of integration – to take high-quality spectra of disks around protostellar objects with masses down to the hydrogen-burning limit and even beyond. Fig. 6 also illustrates how the mid-IR SEDs varies under different boundary conditions and hence can be used as powerful diagnostics for disk evolution and structure, even if the source is spatially unresolved (Armus et al. 2000).

3.3. Example 3: Star Formation in Interacting Galaxies

Collisions between galaxies are one of the most energetic events in the Universe with energies of typically $10^{53}J$ – the equivalent of 10^{8-9} supernovae – on timescales of about 3×10^8 yrs (Struck 1999). The interactions trigger the formation of massive star clusters either directly through the collision of clouds or induce bars which funnel gas and foster wave and resonant ring star formation. The strongest star formation rates are usually observed in the most violently interacting galaxies – the best known example probably is the Antennae galaxy NGC 4038/39.

The young stars within a starburst are extremely enshrouded by dust with typical average extinctions of A_V 25mag (Smith et al. 1996). Hence, observational studies in the mid-IR are the best method to probe the properties of dusty starburst cores and the surrounding interstellar medium. Fig. 7 illustrates the spatial resolution of the IRS spectrographs with their slits overlaid on the

HST/WFPC2 picture of the Antennae galaxy (Whitmore et al. 1999). At the distance of 2.8 kpc the width of the short-high slit ($10 - 21\mu\text{m}$) corresponds to only 500 pc; the length of the short- and long-low slits of $55''$ and $151''$, respectively, make it – for the first time – practically possible to obtain mid-IR spectra of the entire region at relatively high spatial resolution.

Figure 7. The sizes of the IRS short-low (top) and short-high (bottom right) slits projected onto NGC 4038/39. The locations and angles of the slits were arbitrarily chosen.

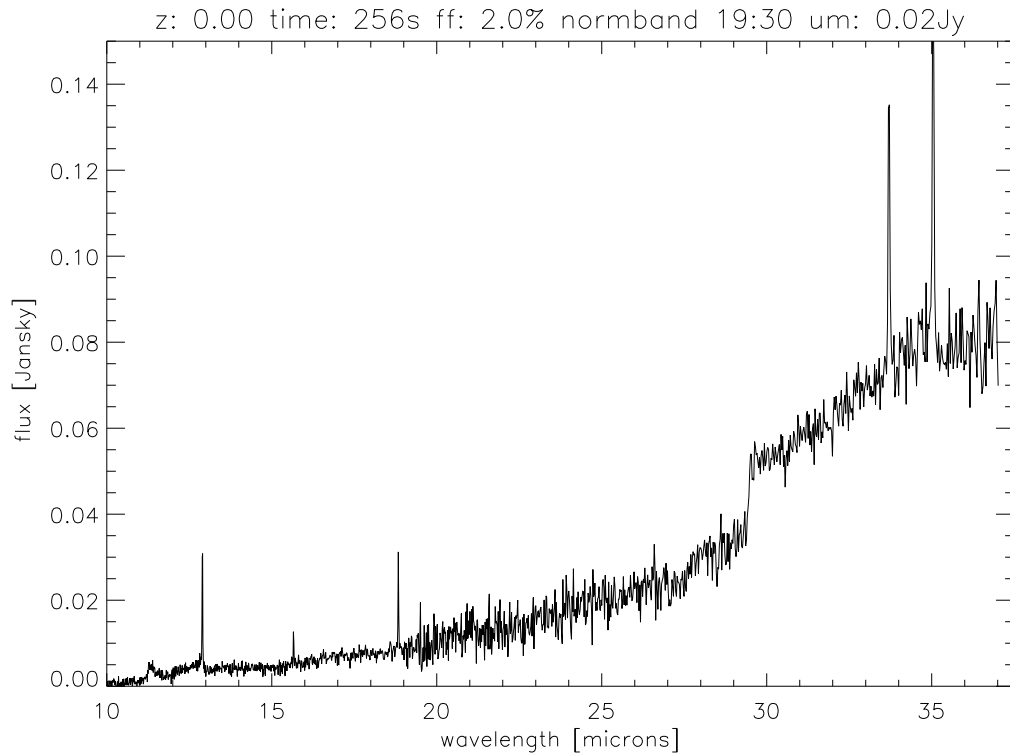


Figure 8. Simulated IRS spectrum of a 20mJy source in 256s integration time per slit, assuming a M82 like spectrum. The most prominent emission lines are: NeII ($12.79\mu\text{m}$), NeIII ($15.55\mu\text{m}$), SIII ($18.71\mu\text{m}$), SIII ($33.48\mu\text{m}$), SiII ($34.80\mu\text{m}$). The “jump” around $30\mu\text{m}$ is due to an artifact in the input spectrum.

Figure 8 shows a simulation of how the spectrum of a low luminosity region in the Antennae galaxy will look when observed with the IRS high-resolution module. The on-source integration time for this simulation is 256s, the flux is normalized to an average 20mJy in the $19 - 30\mu\text{m}$ window, a typical value for a low-luminosity region according to the ISOCAM-CVF map (Mirabel et

al. 1998). The instrument simulation is based on the mid-IR spectrum of the starburst galaxy M82 as observed by ISO-SWS (Sturm et al. 2000). Despite the relative faintness and short integration time one can see a variety of important diagnostic lines (see figure caption).

Acknowledgments. This work was supported under JPL contract 960803.

References

- Allard, F. et al. 1996, ApJ, 465, 123
- Armus, L. et al. 2000, in *The Fourth Tetons Summer Conference: Galactic Structure, Stars, and the Interstellar Medium*, ed. C. Woodward & M.D. Bica, in press
- Brandl, B. et al. 1999, astro-ph/9912216
- Engelbracht, C. et al. 1999, http://mips.as.arizona.edu/MIPS/Science_f.html
- Fanson, J.L. et al. 1998, SPIE 3356, 478
- Fazio, G.G. et al. 1999, in *ASP Conf. Ser. Vol. 177, Astrophysics with Infrared Surveys: A Prelude to SIRTf*, ed. M.D. Bica, R.M. Cutri & B.F. Madore, 462
- Malfait, K. et al. 1998, A&A, 332, 25
- Mirabel, I.F. et al. 1998, A&A, 333, 1
- SIRTf Observers Manual – available from the SSC at <http://sirtf.caltech.edu/SciUser/Documents/SOM.html>
- Smith, D.A. et al. 1996, ApJS, 104, 217
- Struck, C. 1999, Phys. Reports 321, 1
- Sturm, E. et al. 2000, A&A, 358, 481
- Whitmore, B.C. et al. 1999, AJ, 118, 1551

This figure "figure7.jpg" is available in "jpg" format from:

<http://arxiv.org/ps/astro-ph/0007300v1>